

5-2014

# Spatiotemporal Analysis of the January Northern Hemisphere Circumpolar Vortex Over the Contiguous United States

Thomas J. Ballinger

Michael J. Allen

*Old Dominion University*, [mallen@odu.edu](mailto:mallen@odu.edu)

Robert V. Rohli

Follow this and additional works at: [https://digitalcommons.odu.edu/politicalscience\\_geography\\_pubs](https://digitalcommons.odu.edu/politicalscience_geography_pubs)

 Part of the [Atmospheric Sciences Commons](#), [Environmental Studies Commons](#), and the [Geography Commons](#)

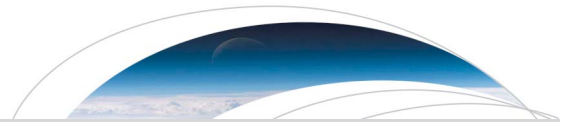
---

## Repository Citation

Ballinger, Thomas J.; Allen, Michael J.; and Rohli, Robert V., "Spatiotemporal Analysis of the January Northern Hemisphere Circumpolar Vortex Over the Contiguous United States" (2014). *Political Science & Geography Faculty Publications*. 1. [https://digitalcommons.odu.edu/politicalscience\\_geography\\_pubs/1](https://digitalcommons.odu.edu/politicalscience_geography_pubs/1)

## Original Publication Citation

Ballinger, T. J., Allen, M. J., & Rohli, R. V. (2014). Spatiotemporal analysis of the January Northern Hemisphere circumpolar vortex over the contiguous United States. *Geophysical Research Letters*, *41*(10), 3602-3608. doi: 10.1002/2014GL060285



## RESEARCH LETTER

10.1002/2014GL060285

## Key Points:

- January 2014 polar vortex over the USA dipped southward but was not extreme
- Teleconnections influence January polar vortex extent and area over the USA

## Supporting Information:

- Readme
- Table S1

## Correspondence to:

T. J. Ballinger,  
tballin1@kent.edu

## Citation:

Ballinger, T. J., M. J. Allen, and R. V. Rohli (2014), Spatiotemporal analysis of the January Northern Hemisphere circumpolar vortex over the contiguous United States, *Geophys. Res. Lett.*, *41*, 3602–3608, doi:10.1002/2014GL060285.

Received 19 APR 2014

Accepted 7 MAY 2014

Accepted article online 12 MAY 2014

Published online 29 MAY 2014

## Spatiotemporal analysis of the January Northern Hemisphere circumpolar vortex over the contiguous United States

Thomas J. Ballinger<sup>1</sup>, Michael J. Allen<sup>1</sup>, and Robert V. Rohli<sup>2</sup>

<sup>1</sup>Department of Geography, Kent State University, Kent, Ohio, USA, <sup>2</sup>Department of Geography and Anthropology, Louisiana State University, Baton Rouge, Louisiana, USA

**Abstract** January 2014 will be remembered for the sensationalized media usage of the term “polar vortex” which coincided with several polar air outbreaks. A United States polar vortex (USPV) perspective is presented to better understand the January spatial and temporal variability of this regional component of the Northern Hemisphere circumpolar vortex. Use of the monthly mean 5460 m isohypse to represent the location of the USPV extent and area revealed that the spatial features of the January 2014 USPV were not extreme relative to certain 1948–2013 Januaries. Furthermore, the Arctic Oscillation (AO), Pacific-North American (PNA) Pattern, and Pacific Decadal Oscillation (PDO) are all linked to southernmost latitude of the USPV trough, but the PDO and PNA are most closely associated with the longitude at which this latitude occurs. The AO is closely related to the area of the United States enclosed within the USPV.

### 1. Introduction

Anomalously cold weather afflicted much of the eastern half of the contiguous United States (CONUS) during January 2014. On 6 January, roughly 50 daily record low temperatures were set at locales across the CONUS stretching from Colorado to New York [*National Aeronautics and Space Administration*, 2014], while on the following day each U.S. state recorded at least one below freezing air temperature, which directly affected power supply and transportation channels from the Midwest to the East Coast and stretching south to the Gulf of Mexico [*Atlanta Associated Press*, 2014]. Low temperatures persisted throughout the month as many states experienced mean January air temperatures rivaling previous records for the month, while Great Lakes collective ice coverage reached 75%, the highest mark observed since 1996 [*National Climatic Data Center (NCDC)*, 2014].

During this time, explanations for the cold outbreaks largely involved the “polar vortex,” a term that became sensationalized and overdramatized by sources of print and visual media. Research examining the mid-tropospheric manifestation of this hemispheric circulation signature, commonly referred to in the climatological research community as the Northern Hemisphere circumpolar vortex (NHCPV), and its large-scale influence on weather and climate, has been conducted for decades [e.g., *Markham*, 1985; *Angell*, 1992; *Davis and Benkovic*, 1992; *Frauenfeld and Davis*, 2003; *Rohli et al.*, 2005; *Wrona and Rohli*, 2007]. However, most of these papers have explored the NHCPV on the hemispheric scale, while regional manifestations of the polar vortex have only been briefly analyzed within the context of these projects.

Given the lack of detailed knowledge about the magnitude of the polar vortex variability across the United States specifically, particularly during the month of January, and the fact that mid-troposphere circulation plays a critical role in directing polar air masses well south into the CONUS during the cold season [e.g., *Rohli and Henderson*, 1998] a United States polar vortex (USPV) perspective is presented. Similar to previous research, the monthly mean shape of the vortex is analyzed with respect to its spatial characteristics, including latitude, longitude, and area, to better understand its spatial and temporal variability over a multidecadal period. Two atmospheric teleconnections (Arctic Oscillation (AO) and Pacific-North American (PNA) Pattern) and one oceanic pattern (Pacific Decadal Oscillation (PDO)), all of which are well known to be linked to Northern Hemisphere-scale mid-tropospheric flow variability, are hypothesized to be related to the USPV extent and area. The AO involves a low-frequency seesaw of atmospheric mass and pressure between the Arctic and the Northern Hemisphere mid-latitudes [*Thompson and Wallace*, 1998]. The PNA Pattern refers to the oscillation of amplitude and phase of the atmospheric ridge-trough configuration with anomalous

ridging (troughing) over the Western Cordillera of North America concurrent with anomalous troughing (ridging) over the southeastern United States [Wallace and Gutzler, 1981]. The PDO is a set of sea surface temperature (SST) anomalies of opposite sign between the northwestern/western/southwestern Pacific and the northeastern Pacific, with shifts in the intensity of the Aleutian Low and attendant circulation features accompanying each extreme phase [Mantua *et al.*, 1997]. Identification of relationships between the AO and PNA versus USPV area will characterize the effectiveness of these indices in measuring the component of the NHCPV over North America. The link between the PDO and USPV variability will improve understanding of how the regional vortex positioning may be impacted by broader-scale, extratropical climatic forcing. The latter is important to consider because the PDO varies considerably on a multidecadal scale [Frauenfeld *et al.*, 2005], while the NHCPV clearly varies annually [Rohli *et al.*, 2005] and intra-annually [Wrona and Rohli, 2007].

## 2. Data

Daily 500 hPa geopotential height data from the National Centers for Environment Prediction/National Center for Atmospheric Research (NCEP/NCAR) first generation reanalysis data set (hereafter NNR) [Kalnay *et al.*, 1996], available from the NOAA/Earth System Research Laboratory (ESRL) Physical Sciences Division, are used to construct the January USPV. The data are analyzed at a 2.5° horizontal resolution across a domain of 20–50°N and 130–65°W in order to capture the entirety of the CONUS. Geopotential height output from NNR has been used extensively in climatic studies across the CONUS and is regarded as a reliable, or Class A, variable since it closely follows observations assimilated into the model [Kalnay *et al.*, 1996]. A rather dense network of upper air observations over the analysis domain dates back to initiation of the reanalysis period [Stickler *et al.*, 2010]. A change in observation times occurred in 1957, but this temporal inhomogeneity does not appear to yield a notable bias in the vortex calculations [Frauenfeld and Davis, 2003]. Therefore, the full record of January mid-tropospheric reanalysis data is employed. Daily data for January months from 1948 to 2014 ( $n = 67$ ) are aggregated to monthly arithmetic mean values. Similar to previous NHCPV studies [e.g., Davis and Benkovic, 1992, 1994; Frauenfeld and Davis, 2003; Rohli *et al.*, 2005], the 5460 m isohypse is chosen to represent the polar vortex because of its tendency to lie near the steepest gradient of atmospheric mass and therefore the primary mid-latitude baroclinic zone [Frauenfeld and Davis, 2003]. The 5460 m isohypse is then contoured for the month of January across the domain.

Three January teleconnection indices, including the AO, PNA, and PDO, are hypothesized to be related to the USPV. The AO, obtained from the Climate Prediction Center (CPC), represents the initial empirical orthogonal function of monthly 1000 hPa geopotential height anomalies poleward of 20°N. The PNA, also collected from CPC, depicts the second rotated principal component of 500 hPa monthly height anomalies from 20 to 90°N. The PDO data, obtained from the Joint Institute for the Study of Atmosphere and Ocean (JISAO) at the University of Washington, describe the principal component of monthly SST north of 20°N. Both CPC-derived teleconnections date back to 1950, while the PDO exists from 1948 onward, and statistical analyses of the indices and USPV characteristics reflect these disparate start dates.

## 3. Methodology

The spatial characteristics of the USPV across the CONUS, including the Great Lakes, are obtained by identifying the latitude (°N) and longitude (°W) of the southernmost extent of the trough defined by the 5460 m isohypse over the CONUS, and calculating the area (km<sup>2</sup>) of the CONUS bounded by a 500 hPa geopotential height less than or equal to 5460 m. In the event that the southern extent for a particular January is located just outside the CONUS (i.e., Pacific/Atlantic Ocean or Canada), the next most southerly point in the CONUS domain that intersects with the 5460 m isohypse is selected for the extent measurements using geospatial functions available in NCAR Command Language version 6.1.2. The extent measurements are calculated on a cylindrical equidistant projection, which accurately depicts distances between the equator and select points (i.e., the USPV isohypse). A pilot analysis revealed negligible differences between latitude and longitude coordinates using the cylindrical equidistant versus cylindrical equal area projections for the first 10 years of reanalysis data (1948–1957), and therefore the former projection is chosen and used to produce the maps.

For area calculations, the ArcGIS 10.1 “kriging” spatial analyst tool was used to interpolate geopotential height values between grid points across the CONUS domain. This tool fits a mathematical function to

**Table 1.** Statistical Metrics of the Location of Southernmost Extent of the January USPV, 1948–2014<sup>a</sup>

Statistical Metrics	Latitude (°N)	Longitude (°W)	Area (10 <sup>6</sup> km <sup>2</sup> )
Mean ( $\mu$ )	43.20	79.74	0.76
Standard deviation ( $\sigma$ )	1.72	11.71	0.42
Maximum (year)	46.48 (1949)	130.00 (1952)	1.95 (1977)
Minimum (year)	38.53 (1977)	67.00 (1968)	0.06 (2005)
Linear trend (yr <sup>-1</sup> )	0.001	-0.162	-0.004
<i>P</i> value	0.918	0.028	0.092

<sup>a</sup>The italicized trend is statistically significant at  $\alpha \leq 0.05$ .

determine the output value for each unmeasured location, thus creating a surface raster. Each raster represents the January geopotential heights for an individual year for a total of 67 interpolated surfaces. The “reclassification” spatial analyst tool is then used to combine values representing the USPV and those representing non-USPV. Rasters were clipped based upon the domain using the “clip raster” data management tool. After converting the raster into a polygon feature, the geometry of the remaining USPV polygon was calculated using the “calculate geometry” tool. The Albers equal area conic projection was selected in order to capture the accuracy of the area measurements. For each year, the January area was calculated and converted to square kilometers (km<sup>2</sup>).

To ensure that the monthly map for January 2014 was indeed representative of the days within the month, kurtosis of the daily distribution of latitude, longitude, and area was examined. Results suggested that longitude varied widely among the days in January 2014, identified by both the high standard deviation and positive kurtosis, but the distributions of both latitude and area are platykurtic. We concluded that the monthly mean height field for January was representative for much of the month, therefore justifying our use of the monthly mean data to place January 2014 in its proper historical perspective.

#### 4. Results

##### 4.1. Examination of USPV Spatial Characteristics

Latitude and (especially) longitude coordinates of the equatorward extent of the USPV boundary are variable across the study period (Table 1). The latitude range is 7.95°, while the longitude range is 63°, with many of the southernmost latitudes and westernmost longitudes occurring prior to 1978. The climatological mean position of the USPV extent is 43.20°N, 79.74°W, near the southwestern edge of Lake Ontario. The northernmost USPV January mean latitude is at 46.48°N, 108.52°W (1949), located over central Montana, while the southernmost latitude is at 38.53°N, 77.50°W, positioned over northeastern Virginia (Figure 1) during the historic winter of 1976–1977 [Diaz and Quayle, 1978; Henson, 2014]. The southernmost USPV

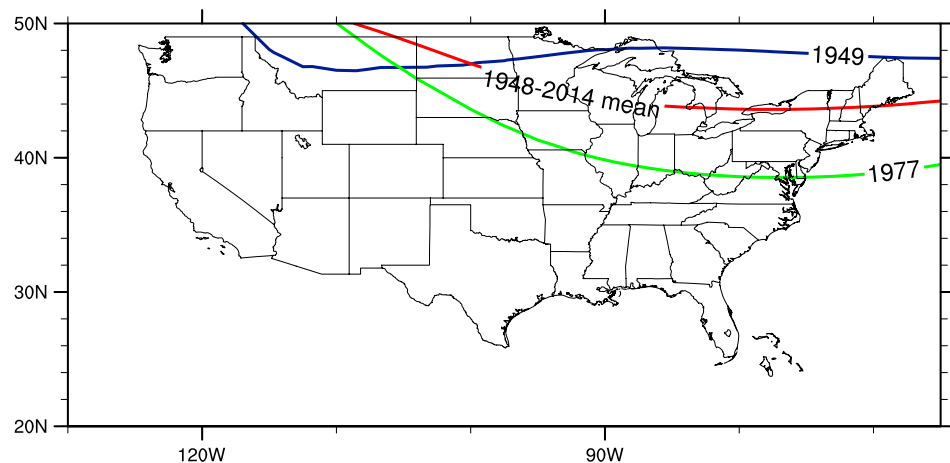


**Figure 1.** USPV maximum (1949), minimum (1977), and mean (1948–2014) latitude plots. For the study period, 1977 is also the maximum area year.

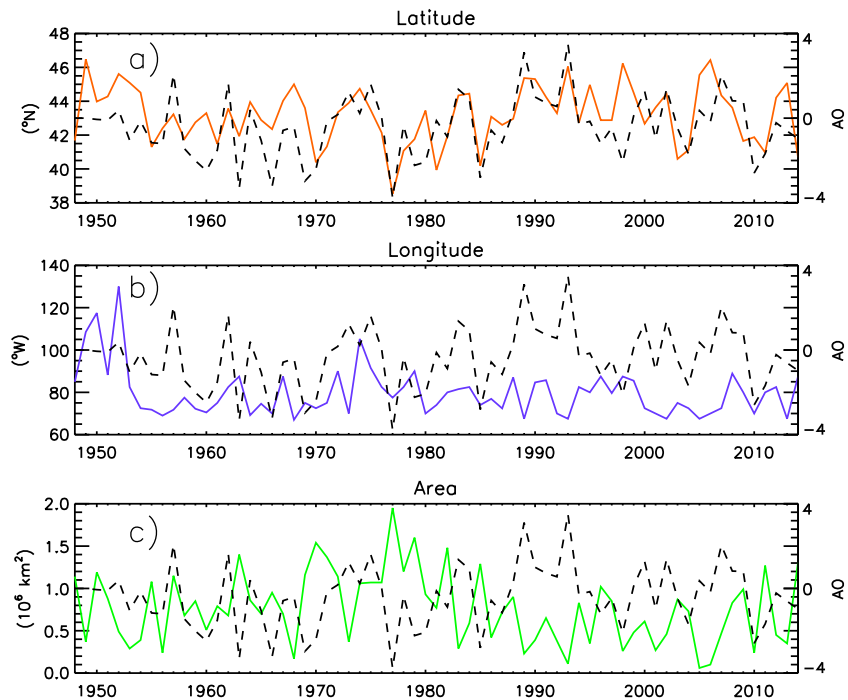


**Figure 2.** January time series of the USPV (a) latitude, (b) longitude, and (c) area and the AO index. The colored lines represent the respective spatial measurements indicated and the dashed black lines represent the AO in each time series.

latitude (observed in 1977) is  $2.72\sigma$  (standard deviations) below the 1948–2014 mean and is  $1.41^\circ$  (or  $\sim 157$  km) from the next southernmost USPV latitudinal position ( $39.94^\circ\text{N}$ ; observed during 1981).

Examining the coordinates separately, the latitude time series (Figure 2a) exhibits a negligible linear trend ( $+0.001^\circ \text{yr}^{-1}$ ,  $p = 0.918$ ) for all January months. Of the six full decades included in the study, the 1970s display the most southerly extent of the USPV for any decade ( $\mu = 42.07^\circ\text{N}$ ), while the highest mean latitudes ( $\mu = 44.31^\circ\text{N}$ ) are found in the 1990s. The variability of the longitudes (Figure 2b), in contrast to that of the latitudes, shows a statistically significant linear trend toward eastward USPV trough movement ( $-0.162^\circ \text{yr}^{-1}$ ,  $p = 0.028$ ). However, this finding appears biased by westward dominant longitudes in the early part of the record; when recalculated from 1953 to 2014 ( $n = 62$ ), no significant trend in USPV was observed ( $+0.013^\circ$ ,  $p = 0.825$ ). January 2014 ranked as the sixth most southerly latitude ( $40.68^\circ\text{N}$ ) and tenth most westerly longitude ( $87.50^\circ\text{W}$ ; Table S1 in the supporting information).

The mean area within the USPV is  $0.76 \times 10^6 \text{ km}^2$  with large fluctuations between maximum and minimum values. The maximum area is observed in 1977 ( $1.95 \times 10^6 \text{ km}^2$ ; Figure 1), when parts of the Northern Plains, Midwest, and Mid-Atlantic and most of the Northeastern United States were within the vortex. This large positive area anomaly is  $2.83\sigma$  above the 1948–2014 climatology and covers roughly a third of a million more kilometers than the next largest area (observed during 1979).

Only a marginally statistically significant linear trend toward decreasing USPV area was observed from 1948 to 2014 ( $-0.004 \times 10^6 \text{ km}^2 \text{ yr}^{-1}$ ,  $p = 0.092$ ). An examination of decadal periods reveals some distinct changes over the time series. In particular, the 1970s decadal mean area ( $\mu = 1.24 \times 10^6 \text{ km}^2$ ) was 36% larger than the next highest decadal value, observed in the 1960s ( $0.79 \times 10^6 \text{ km}^2$ ). The two most recent full decades (i.e., 1990s and 2000s) experienced the smallest mean areas ( $\mu = 0.53 \times 10^6 \text{ km}^2$  and  $0.54 \times 10^6 \text{ km}^2$ , respectively), with the last 5 years (2010–2014) showing some expansion ( $\mu = 0.72 \times 10^6 \text{ km}^2$ ). The five largest January areas occurred during or prior to 1982; a  $t$  test reveals a statistically significant difference between USPV area in the 1948–1982 and 1983–2014 subperiods ( $t = 3.51$ ,  $p = 0.001$ ), supporting the notion that USPV area contracted during most of the last three full decades. January 2014 ranked as the seventh largest area ( $1.31 \times 10^6 \text{ km}^2$ ; Table S1). It remains to be seen whether the 2010–2014 USPV expansion relative to previous decades is indicative of a southward shift similar to that in the 1960s and 1970s.

**Table 2.** Pearson Bivariate Correlations Between the January Teleconnection Indices and the USPV Spatial Properties<sup>a</sup>

Index	Latitude	Longitude	Area
AO	+ <b>0.52</b> (< <b>0.001</b> )	+0.06 (0.662)	- <b>0.42</b> (< <b>0.001</b> )
PDO	-0.26 (0.038)	- <b>0.32</b> ( <b>0.009</b> )	-0.01 (0.919)
PNA	- <b>0.35</b> ( <b>0.003</b> )	-0.30 (0.015)	-0.05 (0.669)

<sup>a</sup>*P* values are noted to the right of the coefficients in the parentheses. Italicized values are statistically significant at  $\alpha \leq 0.05$ , while values in boldface are statistically significant at  $\alpha \leq 0.01$ .

#### 4.2. Regional Teleconnections and USPV Modulations

Past studies have explored relationships between spatial properties of the January polar vortex and teleconnections, albeit using a hemispheric perspective [e.g., Rohli *et al.*, 2005]. Here Pearson bivariate correlations are employed to examine the degree to which the January AO, PDO, and PNA teleconnection indices covary with the USPV spatial properties, thus potentially linking extratropical climatic forcing with the spatial characteristics of the USPV. It is important to note that some overlap exists between these teleconnection indices (particularly the AO and PNA), as they are not orthogonal patterns. Of the aforementioned teleconnections, the January AO index has the strongest and most statistically significant association with properties of the USPV in terms of latitude ( $r = +0.52$ ,  $p = <0.001$ ) and area ( $r = -0.42$ ,  $p = <0.001$ ), but the weakest (insignificant) relationship with longitude (Table 2). The AO and the latitude of the southernmost USPV trough (Figure 2a) appear particularly in-phase throughout parts of the time series, especially from the 1970s through the mid-1990s. During much of this time the AO index exhibited a general increase (i.e., strengthened high latitude lower tropospheric pressure gradient) mirrored by the contraction, or poleward shift, in USPV troughing. The anticorrelation between the AO and USPV area (Figure 2c) suggests that negative AO values coincide with a more amplified, meridional atmospheric flow [Thompson and Wallace, 2001], leading to greater increases of polar air mass intrusions into the middle latitudes. The most extreme negative AO value in 1977 (along with the positive PNA index) suggests notable tropospheric meridionality over the CONUS, coinciding with the USPV latitude minimum and area maximum during that year.

The PNA index shows a statistically significant correlation with the latitude ( $r = -0.35$ ,  $p = 0.003$ ) and longitude ( $r = -0.30$ ,  $p = 0.015$ ) of the USPV. Strong amplification of the 500 hPa ridge-trough configuration (positive index values) directly relates to the USPV latitude positioning of the 5460 m isohypse. For instance, the three highest PNA index values (1977, 1981, and 1985) correspond to the three southernmost USPV extents and decreases (eastward shifts) in longitude values relative to previous years but are not congruent with absolute longitudinal extremes. The significant correlation of the PNA index to latitude and longitude is not surprising, as its definition is based on 500 (and in some applications, 700) hPa geopotential height-based centers of action in northwestern North America and the southeastern United States. More noteworthy is the result that unlike the AO, which is derived from many more geographically fixed centers of action with most beyond North America, there is no significant correlation between the PNA and USPV area. This infers that it is likely that neither a trough-ridge versus ridge-trough configuration, nor an amplified versus deamplified wave train, may differ significantly in the extent of the CONUS falling within the polar vortex.

The PDO also associates well with USPV latitude ( $r = -0.26$ ,  $p = 0.038$ ) and longitude ( $r = -0.32$ ,  $p = 0.009$ ). Positive PDO values (i.e., warm northeastern Pacific and western US coast SST anomalies) coincide with more southern oriented USPV latitudes and longitudes primarily east of 80°W. The Niño 3.4 SST Index [Trenberth, 1997] and the Southern Oscillation Index (SOI) [Chen, 1982], both archived at CPC, were also correlated against the USPV spatial measurements, but neither yielded any significant correlation coefficients. Previous studies have discovered nonsignificant NHCPV area correlations with Niño 3.4 and the SOI and suggested that subareas within the NHCPV may relate more conclusively to these teleconnection indices [e.g., Frauenfeld and Davis, 2000; Rohli *et al.*, 2005]. This paper fails to identify a consistent link between the spatial characteristics of the USPV and these tropical teleconnections, but the potential exists that strong statistical linkages with other regional components of the NHCPV could be found elsewhere.

#### 5. Discussion and Conclusions

Given the recent media attention on the term polar vortex, an updated synoptic perspective of the Northern Hemisphere circumpolar vortex signature over the contiguous United States (USPV) is presented and analyzed.

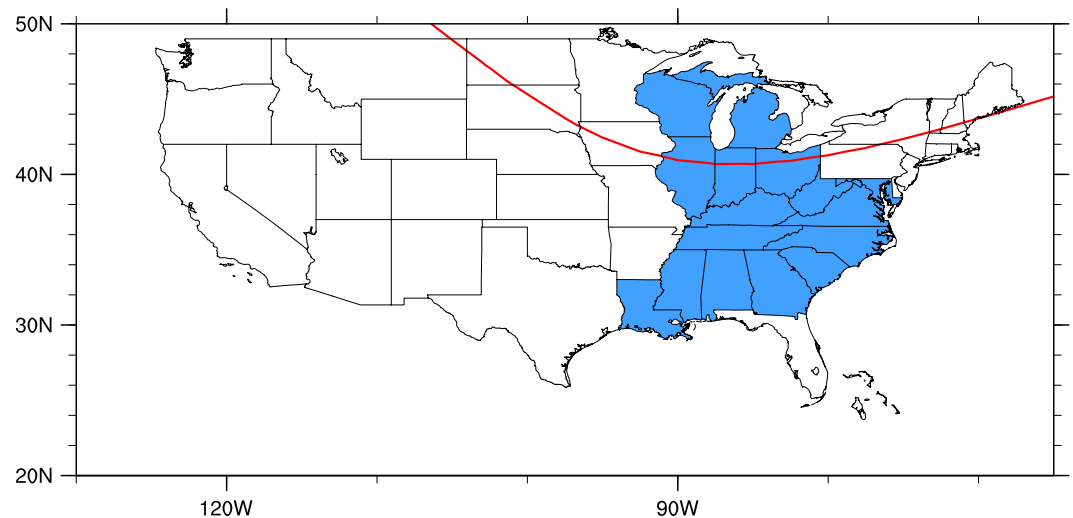


**Figure 3.** The January USPV for 2014 (red contour). States filled in blue recorded statewide January mean surface air temperatures within the coldest 10th percentile for Januarys of the past 120 years [NCDC, 2014].

The 5460 m isohypse, used to define the USPV, shows that other years, such as 1977, were more noteworthy in terms of equatorward latitude extent and area versus those observed in 2014. Specifically, January 2014 ranked as the sixth most southerly latitude ( $40.68^{\circ}\text{N}$ ), tenth most westerly longitude ( $87.50^{\circ}\text{W}$ ), and seventh largest area ( $1.31 \times 10^6 \text{ km}^2$ ; Table S1). Numerous cold air outbreaks across the CONUS, likely steered by the USPV, yielded monthly mean surface air temperatures among the coldest 10% of Januarys on record (in the 120 year history of the National Climatic Data Center Archive) for several Midwestern and Southern states (Figure 3) [NCDC, 2014].

Statistically, significant correlations between the AO, PDO, and PNA teleconnection indices and the USPV indicate that remote atmospheric and oceanic climate variability may be influencing the spatial variability of this regional vortex signature, especially during certain extreme years. This result is consistent with previous research that finds variability in Northern Hemisphere winter upper/middle tropospheric circulation characteristics, such as position and strength, to be physically related to the AO and PNA teleconnections [e.g., Strong and Davis, 2008; Strong and Magnusdottir, 2008]. Other processes, not explored in detail in this study, may also be influencing USPV positioning simultaneously. For instance, Rohli *et al.* [2005] noted a tendency of the NHCPV centroid to occur just north of the Alaskan coast rather than at the North Pole. Modulations of other semipermanent pressure features dominant over the high latitudes, such as the Siberian and Canadian Highs, may also impact the shape of the vortex across the domain.

Previous research has suggested that Arctic sea ice loss during antecedent summers may weaken the temperature gradient and cold season jet stream over North America through anomalous vertical heat transfer from the Arctic Ocean to atmosphere during autumn and early winter [e.g., Serreze *et al.*, 2009], leading to increasingly meridional flow [e.g., Francis *et al.*, 2009; Francis and Vavrus, 2012]. While this USPV study solely examines January, a regional domain, and uses different data to quantify atmospheric circulation, the results presented here are not congruent with the large-scale flow changes suggested in those latter papers. While 2011 and 2014 both rank in the top 10 in terms of largest area and southernmost latitude years since 1948 and follow large Arctic sea ice loss summers (since 1979), other summers of larger boreal areal sea ice decline (2007 and 2012) [National Snow and Ice Data Center, 2014] are not followed by similar anomalous spatial USPV responses during January. Therefore, the addition of future years of data and/or exploration of different monthly aggregations of the USPV may be needed to more critically evaluate the sea ice-January USPV relationship given the definition of the vortex employed in this paper. Future work expanding the temporal basis of analysis to incorporate traditional winter (December-January-February) season regional vortex observations may be enlightening to see how trends manifest over extended interannual periods. Analysis of other middle-latitude regions where the polar vortex intrudes during cold season months may also be worth exploring, especially as related to persistent, anomalous weather conditions collocated with environmental changes.

### Acknowledgments

The authors would like to thank Aaron Wilson (Ohio State University, Polar Meteorology Group), Mary Haley (NCAR, CISL), Jonathan Kirk, Thomas Veldman, Emariana Widner, and Xinyue Ye (Kent State University, Department of Geography) for their assistance with the USPV calculations and figures. Special thanks also to Nate Mantua (JISAO) for promptly updating the January PDO index through January 2014. The NNR data are obtained at the NOAA/ESRL Physical Sciences Division (<http://www.esrl.noaa.gov/psd/data/gridded/data.ncep.reanalysis.html>). AO and PNA indices ([http://www.cpc.ncep.noaa.gov/products/precip/CWlink/daily\\_ao\\_index/teleconnections.shtml](http://www.cpc.ncep.noaa.gov/products/precip/CWlink/daily_ao_index/teleconnections.shtml)) and Niño 3.4 SST Index and SOI (<http://www.cpc.ncep.noaa.gov/data/indices/>) are acquired from the CPC. The PDO index is obtained at the JISAO at the University of Washington (<http://jisao.washington.edu/pdo/PDO.latest>). Recent NCDC monthly temperature data are acquired at <http://www.ncdc.noaa.gov/sotc/national/2014/1>. The authors thank Robert Davis and an anonymous reviewer for their helpful comments.

The Editor thanks Robert Davis and an anonymous reviewer for their assistance in evaluating this paper.

### References

- Angell, J. K. (1992), Relation between 300-mb north polar vortex and equatorial SST, QBO, and sunspot number and the record contraction of the vortex in 1988–1989, *J. Clim.*, *5*, 22–29.
- Atlanta Associated Press (2014), All 50 States saw freezing temperatures at some point Tuesday (January 8, 2014). [Available at <http://atlanta.cbslocal.com/2014/01/08/all-50-states-saw-freezing-temperatures-at-some-point-tuesday/>.]
- Chen, W. Y. (1982), Assessment of Southern Oscillation sea-level pressure indices, *Mon. Weather Rev.*, *110*, 800–807.
- Davis, R. E., and S. R. Benkovic (1992), Climatological variations in the Northern Hemisphere circumpolar vortex in January, *Theor. Appl. Climatol.*, *46*, 63–73.
- Davis, R. E., and S. R. Benkovic (1994), Spatial and temporal variations of the January circumpolar vortex over the Northern Hemisphere, *Int. J. Climatol.*, *14*, 415–428.
- Diaz, H. F., and R. G. Quayle (1978), The 1976–77 winter in the contiguous United States in comparison with past records, *Mon. Weather Rev.*, *106*, 1393–1421.
- Francis, J. A., W. Chan, D. J. Leathers, J. R. Miller, and D. E. Veron (2009), Winter Northern Hemisphere weather patterns remember summer sea-ice extent, *Geophys. Res. Lett.*, *36*, L07503, doi:10.1029/2009GL037274.
- Francis, J. A., and S. J. Vavrus (2012), Evidence linking Arctic amplification to extreme weather in mid-latitudes, *Geophys. Res. Lett.*, *39*, L06801, doi:10.1029/2012GL051000.
- Frauenfeld, O. W., and R. E. Davis (2000), The influence of El Niño–Southern Oscillation events on the Northern Hemisphere 500 hPa circumpolar vortex, *Geophys. Res. Lett.*, *27*, 537–540, doi:10.1029/1999GL010996.
- Frauenfeld, O. W., and R. E. Davis (2003), Northern Hemisphere circumpolar vortex trends and climate change implications, *J. Geophys. Res.*, *108*(D14), 4423, doi:10.1029/2002JD002958.
- Frauenfeld, O. W., R. E. Davis, and M. E. Mann (2005), A distinctly interdecadal signal of Pacific Ocean–atmosphere interaction, *J. Clim.*, *18*, 1709–1718, doi:10.1175/JCLI3367.1.
- Henson, B. (2014), AtmosNews, Perspective: It was so cold! (How cold was it?) (March 5, 2014). [Available at <http://www2.ucar.edu/atmos-news/opinion/11158/it-was-so-cold-how-cold-was-it>.]
- Kalnay, E., et al. (1996), The NCEP/NCAR 40-year reanalysis project, *Bull. Am. Meteorol. Soc.*, *77*, 437–471.
- Mantua, N. J., S. R. Hare, Y. Zhang, J. M. Wallace, and R. C. Francis (1997), A Pacific Interdecadal Climate Oscillation with impacts on salmon production, *Bull. Am. Meteorol. Soc.*, *78*, 1069–1079.
- Markham, C. G. (1985), A quick and direct method for estimating mean monthly global temperatures from 500 mb data, *Prof. Geogr.*, *37*, 72–74.
- National Aeronautics and Space Administration (2014), The big chill (February 18, 2014). [Available at <http://svs.gsfc.nasa.gov/vis/a010000/a011400/a011451/>.]
- National Climatic Data Center (NCDC) (2014), National overview—January 2014. [Available at <http://www.ncdc.noaa.gov/sotc/national/2014/1>.]
- National Snow and Ice Data Center (2014), Arctic sea ice news & analysis, monthly archives, October 2013. [Available at <http://nsidc.org/arcticseaicenews/2013/10/>.]
- Rohli, R. V., and K. G. Henderson (1998), Upper-level steering flow and continental anticyclones on the central Gulf Coast of the United States, *Int. J. Climatol.*, *18*, 935–954.
- Rohli, R. V., K. M. Wrona, and M. J. McHugh (2005), January northern hemisphere circumpolar vortex variability and its relationship with hemispheric temperature and regional teleconnections, *Int. J. Climatol.*, *25*, 1421–1436, doi:10.1002/joc.1204.
- Serreze, M. C., A. P. Barrett, J. C. Stroeve, D. N. Kindig, and M. M. Holland (2009), The emergence of surface-based Arctic amplification, *Cryosphere*, *3*, 11–19.
- Stickler, A., et al. (2010), The comprehensive historical upper-air network, *Bull. Am. Meteorol. Soc.*, *91*, 741–751.
- Strong, C., and R. E. Davis (2008), Variability in the position and strength of winter jet stream cores related to Northern Hemisphere teleconnections, *J. Clim.*, *21*, 584–592, doi:10.1175/2007JCLI1723.1.
- Strong, C., and G. Magnusdottir (2008), Tropospheric Rossby wave breaking and the NAO/NAM, *J. Atmos. Sci.*, *65*, 2861–2876, doi:10.1175/2008jas2632.1.
- Thompson, D. W. J., and J. M. Wallace (1998), The Arctic Oscillation signature in the wintertime geopotential height and temperature fields, *Geophys. Res. Lett.*, *25*, 1297–1300, doi:10.1029/98GL00950.
- Thompson, D. W. J., and J. M. Wallace (2001), Regional climate impacts of the Northern Hemisphere annual mode, *Science*, *293*, 85–89, doi:10.1126/science.1058958.
- Trenberth, K. E. (1997), The definition of El Niño, *Bull. Am. Meteorol. Soc.*, *78*, 2771–2777.
- Wallace, J. M., and D. S. Gutzler (1981), Teleconnections in the geopotential height field during the Northern Hemisphere winter, *Mon. Weather Rev.*, *109*, 784–812.
- Wrona, K. M., and R. V. Rohli (2007), Seasonality of the northern hemisphere circumpolar vortex, *Int. J. Climatol.*, *27*, 697–713, doi:10.1002/joc.1430.